JET-P(96)20

Structural Integrity Assessment of the JET Neutral Beam Components

B D Daniels[1], S Papastergiou.

JET Joint Undertaking, Abingdon, Oxfordshire, OX14 3EA, UK.
[1] AEA Technology plc, Structural Performance Department, Risley.

Preprint of a paper to be submitted for application in proceedings of the International Conference on Life Assessment and Life Extention of Engineering Plant, Structures and Components (Cambridge, Sept 1996)

May 1996

ABSTRACT

Better understanding of the physics involved and possible enhancements have resulted in reappraisal of the high thermal loads and the predicted life of existing copper based components in the Neutral injection system of JET. However, the assessment of high temperature equipment is usually restricted to stainless steel components. The proposed high temperature design rules are based on high temperature criteria defined in the ASME III design code.

BACKGROUND

The Joint European Torus (JET) is the largest project in the co-ordinated fusion programme of the European Atomic Energy Community (EURATOM), whose long term objective is the joint creation of a safe environmentally sound prototype fusion reactor. Construction of the JET machine was completed in 1983, and the machine became operational in June 1983. The JET research programme aims to investigate a number of physics and technological issues in the development of future fusion power stations.

The initial heating of the plasma is produced by ohmic heating. However, the heating effect is reduced as the plasma gets hotter. It is therefore necessary to provide additional heating. The neutral beam system generates a beam of charged particles accelerated to high energies and directed towards the plasma. Since charged particles cannot cross the magnetic field containing the plasma, the beam must be neutralised. The resulting neutral particles cross the magnetic field and give up their energy through collisions to the plasma, thereby raising its temperature. The neutralisation process has a relatively low efficiency (<40%) at the beam energies used (80-140 kV). It is therefore necessary to deflect the residual ion beam and handle large power densities (in the 5-10 MW/m^2 range) on the cooled copper ion dump structures. Other components are also necessary to catch stray reionised beam particles. It is thus necessary to quantify the thermal load effects on these structures

PROBLEM

Better understanding of the physics involved and possible enhancements have resulted in reappraisal of the high thermal loads and the predicted life of existing copper based components in the Neutral injection system of JET.

However, the assessment of high temperature components is usually defined for stainless steel components. The need exists for high temperature design rules for copper based components.

METHODOLOGY

The following design rules applied to the JET components are based on the high temperature assessment criteria in the ASME III design code. The design rules and basic theory are described in detail below.

Elastic Stress Limits

The elastic stress limits are based on the ASME philosophy, to check the overall stress levels. The design stress intensity value (Sm) is the least of either one-third of the ultimate tensile strength at temperature or two-thirds of the yield strength at temperature as defined in ASME II (2). The thermal stresses have been classified using the ASME III classifications (3) as secondary stress (i.e. self-limiting). Local yielding and minor distortion can satisfy the conditions which cause the stress to occur and failure from one application of the stress is not expected (i.e. shake-down). The assessment stresses are compared below to the ASME III stress limits for level-A service requirements (3) for class 1 components.

$$Pm \leq Sm \quad (1)$$

$$Pl \leq 1.5\ Sm \quad (2)$$

$$Pl + Pb \leq 1.5\ Sm \quad (3)$$

$$Pe \leq 3\ Sm \quad (4)$$

$$Pl + Pb + Pe + Q \leq 3\ Sm \quad (5)$$

$$Pl + Pb + Pe + Q + F \leq 2\ Sa \quad (6)$$

Elastic Strain Limits

The possibility of incremental growth of a component subjected to mechanical loading with superimposed thermal cycles may lead to distortion or fracture unless the accumulated inelastic strain is kept within allowable limits. Elastic conditions limit strain to small values but additional criteria are necessary.

The interactive effect of the thermal cycles on the stress distribution within components can be evaluated using a uniaxial model originally proposed by Miller (4) for elastic-plastic behaviour, and redefined by Bree (5) for cyclic load histories. Bree criteria limiting mechanical and thermal stresses eliminate component incremental growth. In the presence of creep, the structure after some cycling develops the so-called steady-state stress cycle.

Steady-State Stress Cycles

The elastic strain limits are based on the assumption that although creep causes the resulting stress field to relax, each thermal cycle subsequent to the relaxation period reinstitutes the original elastic-plastic stress distribution. For shakedown or plastic cycling to exist, a portion of the component wall thickness must remain elastic throughout the life of the component (i.e. elastic core). The stress history of the elastic core can conveniently be used to bound inelastic strains accumulated through-the-wall of the component. The short-term redistribution of stress in the elastic core during the transient does not affect accumulation of inelastic strain, therefore it can simply be disregarded. Creep strains and damage occur only during long-term operation at elevated temperature.

The ratcheting region indicates progressive plastic strain cycling which increases the cumulative plastic strain every cycle. Therefore, the ratcheting process could result in exhaustion of the material ductility and the potential fatigue failure in fewer cycles than would be indicated by fatigue assessment.

BREE Diagram

The accumulated inelastic strains can be bounded, using the results of elastic analysis and the following simple relations derived from equilibrium considerations (Figure 1). Typical stress profiles for characteristic combinations of mechanical stress (σ_p) and cyclic thermal stress (σ_t) values are related to the yield stress (σ_y):

$$\sigma_y = \sigma_p + \sigma_t \tag{7}$$

$$2 \times \sigma_y = \sigma_t \tag{8}$$

$$\sigma_y = \sigma_p + (0.25 \times \sigma_t) \tag{9}$$

$$\sigma_y^2 = \sigma_p \times \sigma_t \tag{10}$$

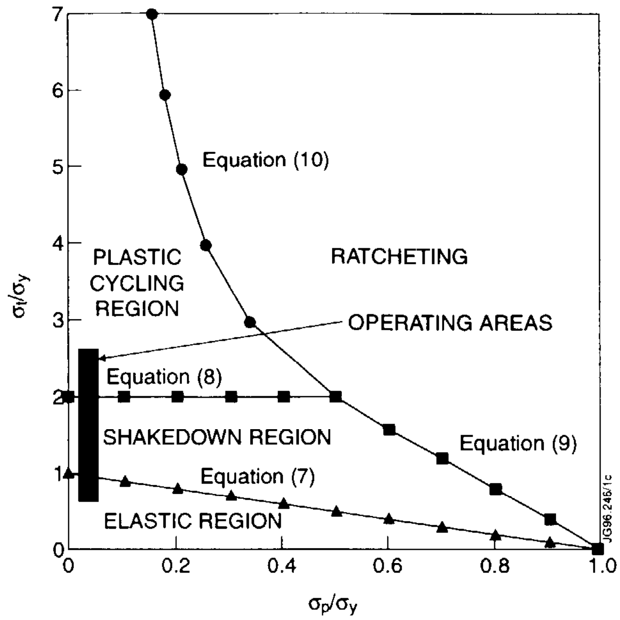

Figure 1 BREE Diagram

Notes

(1) Grids operate in the elastic/shakedown regions.

(2) Duct tiles operate in the elastic, shakedown and plastic cycling regions.

(3) Hypervapotrons operate in the shakedown/plastic cycling regions.

(4) Ratcheting is avoided every where.

APPLICATIONS

Material Properties

The structural integrity assessment of the neutral beam heating duct (Figure 4) is based on the mechanical properties for "oxygen free high conductivity copper" (i.e. nominal composition 99.99% Cu).

Tensile Properties

Tensile properties of pure copper show a steady degradation in strength above 200°C (6). However, the yield strength is sufficient to prevent ratcheting until the temperature is greater than 500°C (i.e. mechanical stress is small). Therefore, the operating temperature should not be greater than 500°C.

Fatigue Life

Measured tensile data has been used to predict fatigue initiation data using the following correlation. This fatigue initiation correlation has been validated for a variety of ductile engineering materials and is reported by Halford and Manson (1). The stress range (2Sa) is related to strain range (Δe) in equation (11). Strain range is related to number of fatigue cycles (N_f) by equation (12).

$$2Sa = \Delta e \times E \qquad (11)$$

$$\Delta e = \left[\frac{3.5 \times \sigma_u}{E} \times N_f^{-0.12}\right] + \left[D^{0.6} \times N_f^{-0.6}\right] \qquad (12)$$

where

$$D = \ln\left[\frac{100}{100 - RA}\right] \qquad (13)$$

Application of this formula has been checked against measured fatigue data for a copper alloy (Cu Cr Zr) by Papastergiou (7) in Figure 2. It is concluded that the fatigue life equation (12) will give a conservative prediction of the fatigue life for copper components.

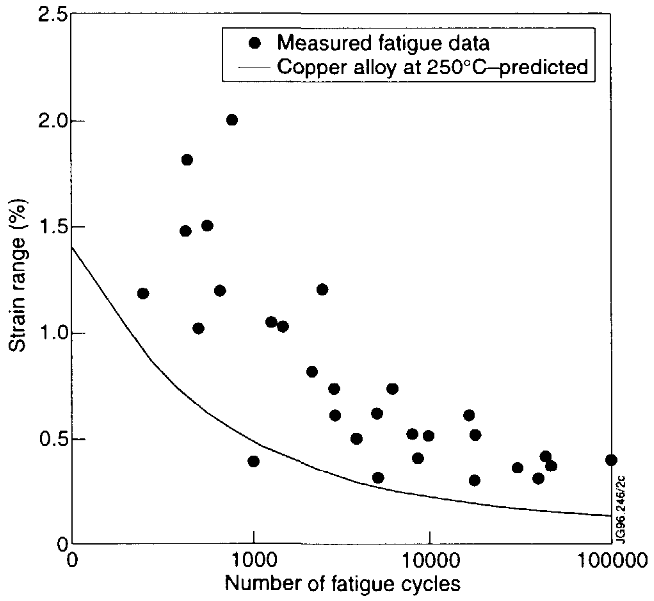

Figure 2 Predicted Fatigue Life for Copper Alloy (Cu Cr Zr)

Examples

The above methodology has been applied to a number of neutral beam heating components including the beam forming grids, duct tiles and hypervapotrons.

Beam Forming Grids

The beam forming grid system consist of four grids which have different electrical potentials that accelerate a beam of ions through the grid holes. During this process the front face of the first grid and the bore of the three following grids receive energy from the high velocity ions.

The neutral beam passing through the holes in the grid provides a heat flux of 200 Watts per hole through the sloping surface of the hole, with an additional flux of 0.1 Watts/cm^2 through the bore surface. Heat is removed from the grid by cooling water passing through channels which run between the holes (Figure 3). Each hole is bounded by four ligaments. Two ligaments are cooled directly by the cooling channels and two are cooled indirectly by conduction only. The radial distribution of the heat flux has been assumed to decrease linearly as the radius increases, with the maximum occurring at the inside edge of the hole.

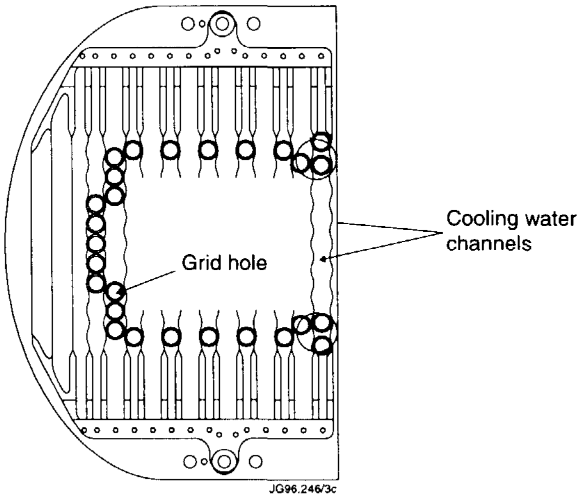

Figure 3 JET Beam Forming Grid

The analysis by Daniels (8) based on conservative assumptions (i.e. tensile behaviour) indicates that the indirectly cooled ligaments are outside the ASME design fatigue life requirement (service level-A) for class 1 nuclear pressure vessels, when fatigue life of 20,000 cycles is required (i.e. Safety factor of only 2 against an ASME safety margin of 20 on cycles). However, the compressive stress cycle will prevent crack opening and therefore stop crack initiation and crack growth. Due to this conservatism and tolerance for fatigue crack growth without coolant leakage, it was concluded that a safety case could be made for operation of the beam forming grid to 20,000 cycles.

Duct Tiles

The neutral heating duct is protected by copper plates mounted on the duct wall (Figure 4). Because the vacuum enclosure through which the beam passes contains a residual gas at low pressure ($\leq 10^{-5}$ mbar) the neutral beam produces (at the 2-3% level) ionised particles which are transported to the copper plates by the magnetic field thus, the possibility of reionisation heating of the tiles has to be taken into account. Thermal energies of 3KJ/cm^2 to 7 KJ/cm^2 and power densities of 300 W/cm^2 to 800 W/cm^2 can be applied. The analysis by Daniels (9) has demonstrated that the front surface temperature of 500°C is the limiting factor because of significant material property changes above that temperature. Some crack initiation and propagation may occur prior to reaching the temperature limit, but due to the very low mechanical stress (i.e. non-thermal stress) there is no major concern for ~10,000 identical cycles.

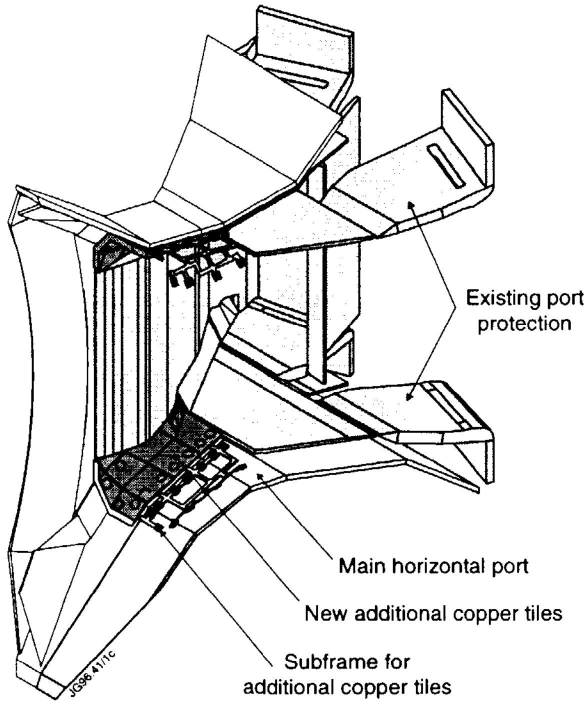

Figure 4 JET Neutral Beam Injection Duct

Hypervapotrons

These elements (Figure 5) are used to remove large heat fluxes under steady state conditions from the JET ion dumps. Stable boiling heat transfer occurs with heat transfer coefficients of up to 100 $KW/m^2.{}^{\circ}C$. The structural integrity of the JET Hypervapotron for power densities up to 50% above design value (i.e. up to 12 MW/m^2, with relatively modest flow velocity of ~4 m/s) has been examined by Daniels (10). It appears again that a limit of 450°C for the front surface temperature of the element is acceptable and compatible with the enhanced power loading despite relatively large strains which are predicted.

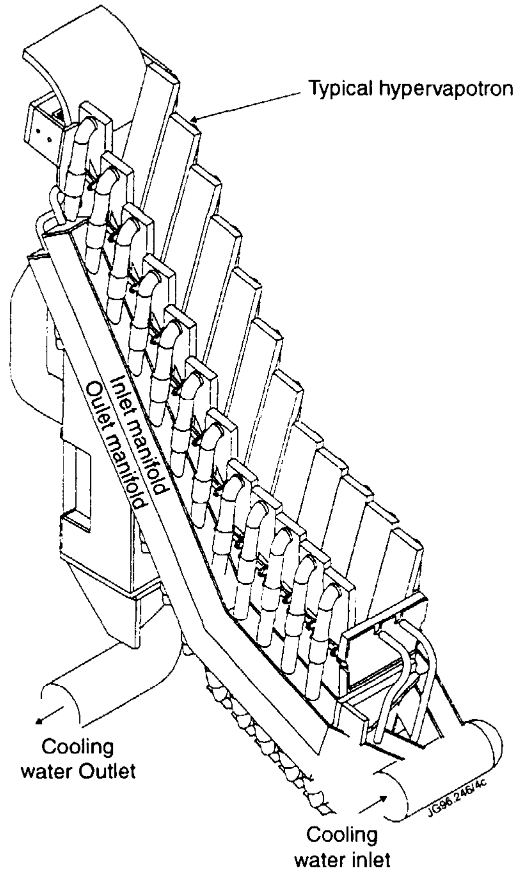

Figure 5 General Arrangement of the JET Ion Dump

CONCLUSIONS

The high temperature design rules as defined by ASME have been applied successfully to a number of neutral beam heating components including the beam forming grids, duct tiles and hypervapotrons. As a result of the above analysis it has be demonstrated that the neutral beam system may be safely upgraded to increase the injected power. The BREE diagram (Figure 1) indicates the operating areas of all the components examined. Ratcheting is avoided.

SYMBOLS USED

Δe = total strain range

N_f = number of cycles to failure

D = true tensile ductility (equation (12))

σ_u = ultimate tensile strength (MPa)

E = modulus of elasticity (MPa)

RA = percentage reduction in area (%)

Pm = general primary membrane stress due to mechanical loads (MPa)

Pl = local primary membrane stress due to mechanical loads (MPa)

Pb = primary bending stress due to mechanical loads (MPa)

Pe = thermal membrane stress (MPa)

Q = secondary stress due to thermal loads (MPa)

F = peak stress due to stress concentration effects (MPa)

Sm = design stress intensity (MPa)

Sa = allowable stress amplitude (MPa)

σ_p = mechanical stress

σ_t = thermal stress

σ_y = yield stress

REFERENCES

1. Halford, G.R. and Manson, S.S. "Application of a method of estimating high-temperature low-cycles fatigue behaviour of materials", ASME Transactions Volume 61, 1965.
2. ASME II, Materials, Part D - Properties 1992 Edition.
3. ASME III Division 1 - Subsection NB Class 1 components, 1992 Edition.
4. Miller, D.R. "Thermal-stress ratchet mechanism in pressure vessels", Transactions ASME, Vol. 81, 1959, p. 190.
5. Bree, J. "Elastic-plastic behaviour of thin tubes subjected to internal pressure and intermittent high-heat fluxes with application to fast nuclear reactor fuel elements", Journal of strain analysis, Vol. 2, 1967, p. 226.
6. Karditsas, P.J. and Baptiste, M-J "Thermal and structural properties of fusion related materials", UKAEA Government division, Fusion (UKAEA/Euratom Fusion Association), UKAEA FUS 294, 1995.
7. Papastergiou, S. "Summary of available copper fatigue test data", Private communication, 1996.
8. Daniels, B.D., Curbishley, I. & Richardson, T. "Structural integrity assessment of the JET beam forming grid 1", SPD/D(94)344, 1995.
9. Daniels, B.D., Sherry, A., Richardson, T. and Papastergiou, S. "Structural integrity assessment of the JET duct scraper", SPD/D(95)460, 1995.
10. Daniels, B.D., Richardson, T. and Papastergiou, S. "Structural integrity assessment of the JET Hypervapotron", SPD/D(95)521, 1996.